Kovove Mater. 49 2011 385–391
DOI: 10.4149/km_2011_6_385

Effect of fabrication processing on the deformation behaviour of AZ31 magnesium alloys

P. Lukáč*, J. Balík, Z. Trojanová

Department of Physics of Materials, Faculty of Mathematics and Physics, Charles University, Ke Karlovu 5, 121 16 Prague 2, Czech Republic

Received 9 August 2011, revised 19 September 2011, accepted 23 September 2011

Abstract

The influence of two fabrication techniques – cast and rolling – on the deformation behaviour of Mg-3Al-1Zn (AZ31) alloys was investigated. The tensile tests were conducted over a wide temperature range of 25 and 300 °C at a constant strain rate. The rolled (textured) samples exhibit a strong basal texture – the flow stress depends on the orientation of the tensile to the rolling direction. It is shown that the deformation behaviour of AZ31 alloy polycrystals depends on their microstructure produced by processing and temperature. The values of the yield stress, flow stress and maximum stress of the AZ31 sheets are significantly higher than those of the AZ31 cast alloy if samples are deformed at room temperature, whereas the difference in the stress values for both types of samples is insignificant if deformed at 300 °C. The plots of the strain hardening rate against flow stress for the AZ31 sheets indicate interactions between basal and non-basal dislocations. The values of internal stress decrease with increasing deformation temperature, which indicates that recovery processes play an important role during deformation at higher temperatures. The activity of two deformation mechanisms is considered: (a) interaction between dislocations moving in basal and non-basal slip systems producing sessile and glide dislocations, which leads to hardening and (b) cross slip of dislocations through prismatic planes causing softening.

Key words: magnesium alloys, AZ31, dislocation motion, mechanical properties

1. Introduction

Owing to their low density, high specific strength at room temperature, good damping and recyclability, magnesium alloys are very attractive for various applications. On the other hand, the yield strength and ultimate tensile strength of many magnesium alloys decrease rapidly with increasing temperature; at elevated temperatures they are poor. Disadvantages of magnesium alloys are their low ductility and limited formability connected with the hexagonal close-packed (hcp) crystal structure. The main (easy) glide system in Mg and its alloys is the basal slip system, i.e. motion of <**a**> dislocations in the basal plane in one of two independent directions. However, five independent deformation modes are necessary for homogeneous plastic deformation of a polycrystal, according to the von Mises criterion [1]. An improvement in ductility may be owing to the activity of non-basal slip systems and/or deformation twinning [2–5]. Twinning may also accommodate strain along the c axis. Among non-basal slip systems, prismatic and second-order pyramidal slip systems are often considered. The second-order pyramidal slip systems, $\{11\bar{2}2\}$ $\langle 11\bar{2}3\rangle$, that have dislocations with the Burgers vector <**c** + **a**>, offer five independent slip systems. The activity of a non-basal slip system depends on its critical resolved shear stress (CRSS). The CRSS for non-basal slips at room temperature are much higher than that for basal slip. However, they decrease very rapidly with increasing temperature. Therefore, the activity of second-order pyramidal slip systems with glide of <**c** + **a**> dislocations is expected to be easier at elevated temperatures.

Only few studies are dealing with investigations

*Corresponding author: tel.:+420 221911366; fax: +420 221911490; e-mail address: lukac@met.mff.cuni.cz

of the deformation behaviour of magnesium alloys at different temperatures. These studies enable to estimate not only the temperature dependences of the yield stress and tensile strength, as important characteristics, but also to determine the dislocation mechanisms responsible for the deformation behaviour. It is widely accepted [6] that the resolved shear stress, τ, necessary for dislocation motion in the slip plane can be divided into two components: the athermal (called also internal) stress, τ_i, and the effective shear stress (often called thermal), τ^* . In polycrystal deformation, the applied stress is related to the resolved shear stress as $\sigma = M\tau$, where M is the Taylor factor. It should be mentioned that the value of the Taylor factor for magnesium alloys depends on the sample texture [7]. One may write the flow stress and its components:

$$\sigma = \sigma_\mathrm{i} + \sigma^*. \tag{1}$$

The (internal) athermal contribution to the stress results from long-range internal stress fields impeding the plastic flow. The effective stress σ^* acts on dislocations during their thermally activated motion when they overcome short range obstacles. The plastic strain rate $\dot{\varepsilon}$ for a single thermally activated process can be expressed as:

$$\dot{\varepsilon} = \dot{\varepsilon}_0 \exp\left[-\Delta G(\sigma^*)/kT\right], \tag{2}$$

where ε_0 is a pre-exponential factor containing the mobile dislocation density, the average area covered by the dislocations in each activation act, the Burgers vector of dislocations, the vibration frequency of the dislocation line, and the geometric factor. T is the absolute temperature and k is the Boltzmann constant. $\Delta G(\sigma^*)$ is the change in the Gibbs free enthalpy depending on the effective stress $\sigma^* = \sigma - \sigma_\mathrm{i}$ and its simple form is

$$\Delta G(\sigma^*) = \Delta G_0 - V\sigma^* = \Delta G_0 - V(\sigma - \sigma_\mathrm{i}). \tag{3}$$

Here ΔG_0 is the Gibbs free enthalpy necessary for overcoming a short-range obstacle without the stress and $V = bwL$ is the activation volume, where b is the Burgers vector, w is the obstacle width and L is the mean length of dislocation segments between obstacles. It should be mentioned that L may depend on the stress acting on dislocation segments. It should be noted that the stress-strain curves of a polycrystal deformed at various temperatures are significantly influenced by storage and annihilation of dislocations and changes in the texture.

The aim of this paper is to study the effect of two different fabrication routes on the deformation behaviour of AZ31 magnesium alloy in a wide temperature range and to describe dislocation mechanisms controlling the behaviour. The results could get a better insight in the strain hardening at different temperatures.

2. Experimental procedure

In this work the material for investigation was prepared from AZ31 magnesium alloy (nominal composition in mass%: 3 Al, 0.8 Zn, 0.2 Mn) by two different fabrication routes: a) casting and b) warm-rolled conditions. Samples of cast alloy for tensile tests having a cylindrical form with a diameter of 5 mm and a gauge length of 25 mm were deformed using an INSTRON tensile machine at a constant cross head speed giving an initial strain rate of $6.7 \times 10^{-5}\,\mathrm{s}^{-1}$. The microstructure of the cast alloy was homogeneous with an average grain size of 250 μm. The AZ31 sheets were in the stress-relieved (H24) temper – annealed at 150 °C for 1 h (hereafter referred to as H24 or H). Tensile specimens of AZ31 sheets with a gauge length of 25 mm, 5 mm width and 1.6 mm thickness were also deformed in an INSTRON tensile machine at an initial strain rate of $1.3 \times 10^{-3}\,\mathrm{s}^{-1}$. It should be noted that in the case of AZ31 alloy deformed at room temperature, a strain rate increase of one order causes an increase in the yield strength of 1 to 1.5 MPa. The mean grain size of the AZ31 H24 sheets was 45 μm. Some sheet specimens were annealed at 300 °C for 8 h in order to obtain an alternative state with the lower preliminary hardening due to stored dislocations and twin boundaries (hereafter referred to as 300/8 or A). The resulting microstructure appears highly uniform, equiaxed with a grain size of 15 μm and free of twins. For sheet specimens, tensile tests with load axis parallel (hereafter R specimens) to the rolling direction were conducted. Tensile tests were carried out at various temperatures between room temperature and 300 or 400 °C. The temperature in furnace was controlled to within ± 2 °C.

3. Results and discussion

The rolled AZ31 sheets exhibit a strong basal texture as shown in previous papers [8, 9]. The true stress-true strain curves for the cast AZ31 alloy obtained in tension at different temperatures are presented in Fig. 1. The true stress-true strain curves of the AZ31 sheets in the H24 condition with the tensile axis parallel to the rolling direction obtained at various temperatures are given in Fig. 2 – reproduced from [9]. In the same Fig. 2, the true stress-true strain curves for annealed AZ31 sheets are also presented. It can be seen that the testing temperature influences strongly the deformation behaviour. The shape of the true stress-true strain curves of specimens prepared by both processing routes is very sensitive to the testing temper-

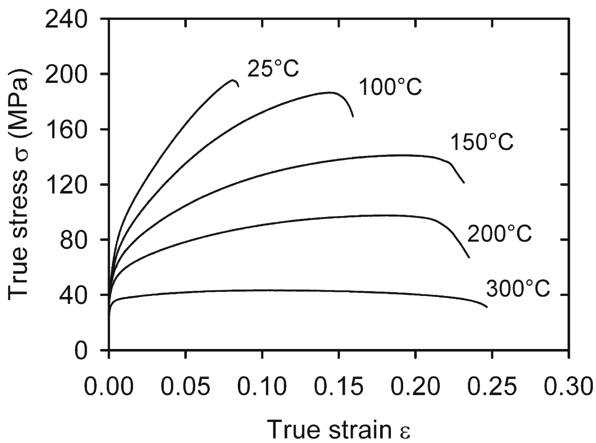

Fig. 1. True stress-true strain curves for the AZ31 cast alloy at different testing temperatures.

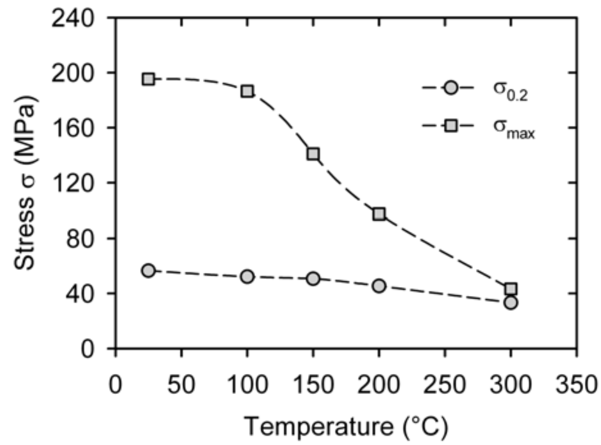

Fig. 3. Temperature dependence of the yield strength and maximum stress for the AZ31 cast alloy.

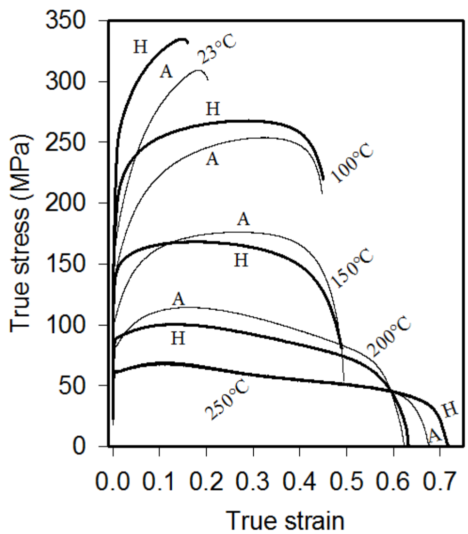

Fig. 2. True stress-true strain curves for the sheets in the H24 state (denoted H) and after annealing at 300 ℃ for 8 h (denoted A). Samples were deformed at different temperatures with the tensile axis parallel to the rolling direction [9].

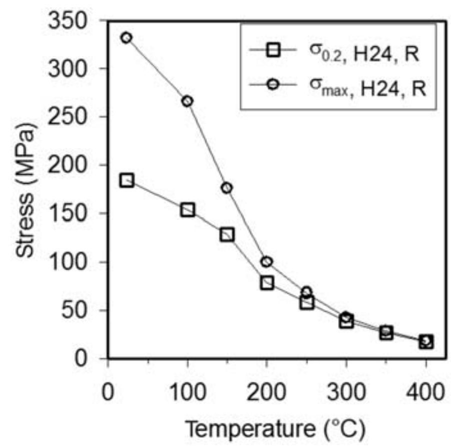

Fig. 4. Temperature dependence of the yield strength and maximum stress for the AZ31 sheets in the H24 state deformed with the tensile axis parallel to the rolling direction [9].

ature. The flow stress decreases and the elongation to fracture increases with increasing temperature. The strain hardening effect of both specimen types is also influenced by temperature. At higher temperatures, above about 200 to 250 ℃, the flow stress is practically independent of strain, i.e. no significant strain hardening is observed. Softening occurs at higher strains for testing at elevated temperatures. It can also be seen that processing methods influence the value of the flow stress.

The yield strength, $\sigma_{0.2}$, determined as the flow stress at 0.2 % offset strain and the maximum flow stress, $\sigma_{\max}$, determined as the maximum flow stress are plotted against temperature in Figs. 3 and 4 [9] for the cast AZ31 and the AZ31 sheets, respectively. Figure 3 shows a moderate decrease of the yield strength and a rapid decrease of the maximum stress of AZ31 specimens prepared from cast ingots. On the other hand, both the yield strength and the maximum stress of AZ31 sheets decrease rapidly with a temperature increase. The values of both the yield stress and maximum stress for the annealed AZ31 sheets are lower if the specimens are deformed between room temperature and 150 ℃ [9]. It can be seen that the values of the yield stress and maximum stress for the AZ31 sheets are much higher than those of the cast AZ31 samples deformed at the same temperature as expected. The difference between the yield stress of the sheets deformed at room temperature and that of the cast specimens is about 130 MPa whereas the difference of the same stresses for specimens deformed at 300 ℃ is insignificant. The value of the yield stress is influenced by the grain size, the dislocation density and texture. The stress required to the polycrystal deformation depends on the grain size according to the well-known Hall-Petch relation [10, 11]:

$$\sigma_{0.2} = \sigma_0 + k_0 d^{-1/2}, \tag{4}$$

where σ_0 is a constant (the extrapolation to the stress axis) and the slop k_0 depends on the material investigated and on the testing temperature. The values of k_0 vary over a wide range (see e.g. [12–14]). One can calculate the difference between the yield stresses of the sheets and the cast specimens due to the different grain sizes using Eq. (4); it has a value between 30 and 40 MPa depending on the value of k_0 [12, 14]. It is clear that an increase in the yield strength of the sheets in comparison to the cast specimens cannot be accounted for only by the grain size difference. It should be considered texture and first of all a higher dislocation density in the sheets duo to their fabrication (rolling) route. It is obvious that the dislocation contribution may be estimated according to the well-known relationship between the stress and the total dislocation density, ρ, in the following form:

$$\sigma = M\alpha G b \rho^{1/2}, \tag{5}$$

where α is a constant, G is the shear modulus and b is the Burgers vector. Using (5) one can estimate an increase in the total dislocation density in the sheets due to rolling to be about 7–10 times higher than in the cast specimens. It is interesting to note that the difference between the maximum stress (ultimate tensile strength) and the yield strength at room temperature is practically identical for both specimen types, it is about 150 MPa. Zuberova et al. [15] investigated the effect of the deformation processing on tensile ductility of AZ31 magnesium alloy deformed at room temperature. They showed that the grain size was reduced and the yield stress increased after hot cross rolling in comparison to coarse grained specimens prepared by squeeze casting. The difference in the yield stresses was about 130 MPa. They did not study the deformation behaviour at different temperatures. Balík et al. [9] have reported that the values of the yield strength of the AZ31 sheets after annealing at 300 ℃ for 8 h are lower than those of the AZ31 sheets deformed without annealing. We believe that this difference was caused by a decrease of the dislocation density and the volume fraction of twins. It has been also reported that the flow stress of the AZ31 sheets deformed with the tensile axis perpendicular to the rolling direction was higher than that for specimens deformed in the rolling direction [9].

In contrast to the different values of the yield strength (and the maximum stress) of the specimens prepared by both fabrication routes, the shapes of the true stress-true strain curves are very similar for the both specimen types. The deformation behaviour is significantly influenced by temperature. The results demonstrate that the effect of temperature on the deformation behaviour of the both specimen types is qualitatively the same. It should be mentioned that similar stress-strain curves as in this work have been reported for magnesium alloys AX41, AX91, AJ51 and AJ91 processed by the squeeze cast technique and deformed in tension and compression at different temperatures between room temperature and 300 ℃ [16].

It can be seen that the flow stress and the strain hardening rate change with strain and temperature (Figs. 1 and 3). At temperatures above about 200–250 ℃, the flow stress is practically independent of strain or decreases with strain at higher strains. The strain hardening rate is very close to zero. It means that hardening is compensated for by dynamic recovery. It should be taken into account both hardening and softening during straining. In tests at elevated temperatures, we did not observe any change in the grain size during straining. Thus, we may assume that changes in the flow stress and the strain hardening rate are caused due to changes in the total dislocation density with strain and temperature during plastic deformation. Therefore we may assume that the athermal (internal) component of the flow stress, σ_i, depends on the total dislocation density, ρ, according to Eq. (5). Glide dislocations stored at obstacles create long-range stress fields and therefore contribute to hardening. On the other hand, moving dislocations may cross slip and/or climb. After double cross slip and/or climb, dislocations may annihilate and hence, the total dislocation density decreases, which causes a decrease in the strain hardening – dynamic recovery (and/or dynamic recrystallization) may take place. The activity of cross slip and climb is strongly influenced by the testing temperature. The total dislocation density should decrease with an increase in the testing temperature. Under some test conditions, a dynamic balance between hardening and softening may occur. Figure 5 shows the temperature variation of the internal/applied stress ratio obtained from the stress relaxation tests at a strain of 0.01 (at the very beginning of plastic deformation). The stress relaxation tests and the method how to estimate the internal stress component are described by Trojanová and Lukáč [16]. The internal stress component is about 95 % of the applied stress of the AZ31 cast alloy deformed at room temperature. Preliminary results obtained for the AZ31 sheets show that the internal stress component is about 89 % of the applied stress. From Fig. 5 it is obvious that the internal stress component decreases with increasing temperature. It means the total dislocation density decreases with an increase in the testing temperature, which is connected, as we expect, with a growing intensity of softening

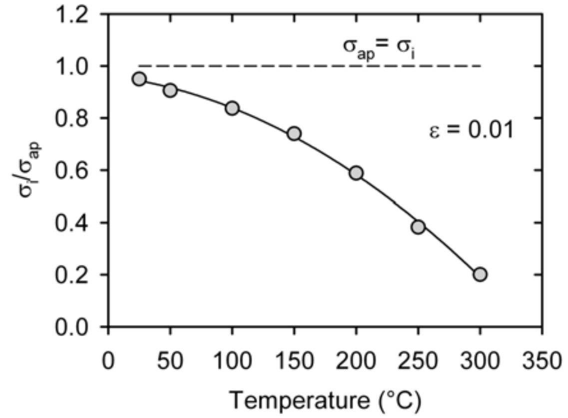

Fig. 5. Temperature variation of the internal/applied stress ratio obtained from the first stress relaxation test at the beginning of strain estimated for the AZ31 cast alloy.

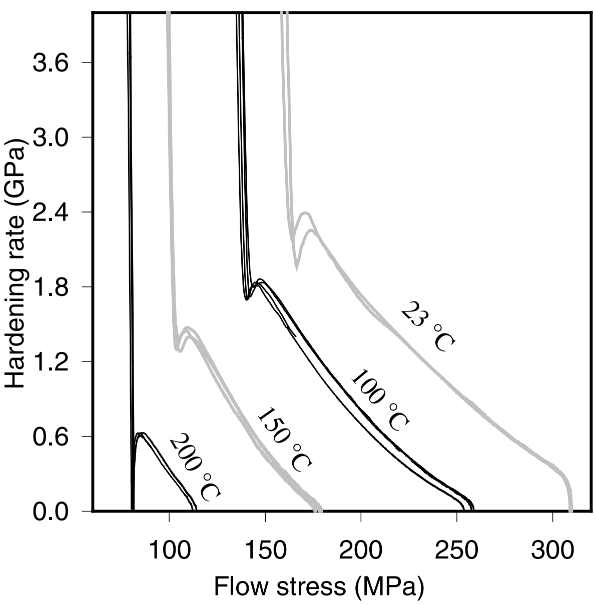

Fig. 6. Stress dependence of the strain hardening rate at different temperatures for the AZ31 sheets deformed after annealing at 300 °C for 8 h.

mechanisms leading to a decrease in strain hardening, as observed experimentally (Figs. 1 and 3).

The strain hardening behaviour may be analysed using a plot of the strain hardening rate, θ, against the flow stress. This is shown in Fig. 6 for specimens in an annealing state deformed at different temperatures. Figure 7 shows the strain dependence of the strain hardening rate. The experiments were repeated – the θ vs. σ curves (Figs. 6 and 7) exhibit insignificant scatter. It can be seen that in the early straining stages, the strain hardening rate first decreases, then increases and after an increase again decreases with increasing stress (and strain). The θ vs. σ and also θ

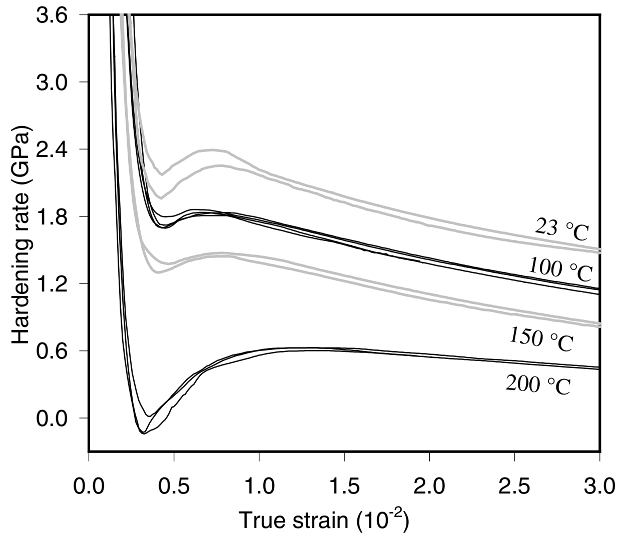

Fig. 7. Strain dependence of the strain hardening rate at different temperatures for the AZ31 sheets deformed after annealing at 300 °C for 8 h.

vs. ε plots for the 300/8 AZ31 sheets are accompanied by a lift in the strain hardening rate. The lifts were observed independent of the tensile direction with respect to the rolling direction. They were not observed for the AZ31 sheets in the H24 state [8]. We assume that these lifts are connected with the activity of a non-basal slip rather than twinning – they are related to the transition from basal (primary) to a non-basal (secondary) slip. The activity of double prismatic slip is very probable. The activities of non-basal slip systems play an important role in both hardening and softening processes.

The activity of the non-basal slip systems such as prismatic and pyramidal slip systems (as well as twinning) are considered as conditions for plastic deformation of polycrystalline magnesium and its alloys, e.g. [4, 5]. However, their activities based on the dislocation theory are rarely taken into account [2, 3, 17–19]. $\{10\bar{1}2\}$ twinning and $\{11\bar{2}2\}$ $\langle 11\bar{2}3\rangle$ second-order pyramidal slip system allow the macroscopic strain along the c axis. Moving dislocations in the basal plane – <**a**> dislocations – may interact with the dislocations in the pyramidal slip systems – <**c** + **a**> dislocations. Different dislocation reactions can occur [2, 3, 9]. The following reactions are important:

$$\frac{1}{3}\langle 2\bar{1}\bar{1}3\rangle_{\mathrm{g}} + \frac{1}{3}\langle \bar{2}110\rangle_{\mathrm{g}} \rightarrow \langle 0001\rangle_{\mathrm{s}}\,. \qquad (6)$$

Gliding dislocations (glissile) in pyramidal planes meet gliding dislocations in the basal planes and immobile (sessile) <**c**> dislocations may arise within the basal planes. Another dislocation reaction between gliding pyramidal dislocations and the basal <**a**> dislocation produces a sessile <**c** + **a**> dislocation according to the reaction:

$$\frac{1}{3}\langle 2\bar{1}\bar{1}3\rangle_{\mathrm{g}} + \frac{1}{3}\langle \bar{1}2\bar{1}0\rangle_{\mathrm{g}} \rightarrow \frac{1}{3}\langle 11\bar{2}3\rangle_{\mathrm{s}}. \tag{7}$$

Two glissile <**c** + **a**> dislocations may interact according to the reaction:

$$\frac{1}{3}\langle 2\bar{1}\bar{1}3\rangle_{\mathrm{g}} + \frac{1}{3}\langle \bar{1}2\bar{1}\bar{3}\rangle \rightarrow \frac{1}{3}\langle 11\bar{2}0\rangle_{\mathrm{s}}. \tag{8}$$

A sessile dislocation of <**a**> type is produced. It is situated along the intersection of the second-order pyramidal planes. The subscript g and s in the reactions denotes glissile (moving) and sessile (immobile) dislocation, respectively.

It is obvious from the dislocation reactions that the interactions between <**c** + **a**> and <**a**> dislocations may produce both sessile and glissile dislocations. Therefore the glide of <**c** + **a**> dislocations is responsible for strain hardening because immobile or sessile dislocations – obstacles for moving dislocation – may be created. On the other hand, the activity of the second-order pyramidal slip systems with the gliding <**c** + **a**> dislocations may contribute to softening because mobile or glissile dislocations can also be formed. The activation of the pyramidal slip systems is possible if the resolved shear stress in the system reaches a critical stress. It is important to mention that the critical value of the stress for the system activation may be lower than the critical resolved shear stress for the non-basal slip system in single crystal considering the fact that the stress concentration at the head of the dislocation pile-ups formed at grain boundaries (they are also obstacles for moving dislocations) decreases the resolved shear stress necessary for the activity of non-basal slip systems. The resolved shear stress is decreasing with increasing temperature. An increase in the activity of non-basal slip systems with increasing temperature contributes to the enhanced ductility observed with the temperature increase. In this connection should be mentioned that Máthis et al. [20] who studied the evolution of non--basal dislocations as a function of temperature have reported that at higher temperatures the fraction of <**c** + **a**> dislocations increased at the cost of <**a**> type dislocations.

On the other hand, screw components of both <**a**> and <**c** + **a**> dislocations may move to the parallel slip planes by double cross slip through prismatic and/or first-order pyramidal planes. After the double cross slip, dislocations can annihilate, which leads to softening. Couret and Caillard [21, 22] who investigated motion of dislocations in Mg single crystal oriented for prismatic slip using in-situ TEM experiments concluded that dislocations were more mobile in the basal plane than in the prismatic ones. They claimed that the mobility of screw components of <**a**> dislocations was much lower than that of edge components and therefore the deformation in prismatic planes was controlled by thermally activated glide of the screw segments. A fraction of dislocations may also be annihilated by climb of dislocations with jogs with help of pipe diffusion. The activity of both cross slip and climb increases with increasing temperature. The effect of both cross slip and climb of dislocations on the stress dependence of the strain hardening rate were considered by Lukáč and Balík [23].

4. Conclusions

The strain hardening behaviour of the cast AZ31 alloy samples and AZ31 sheets in the H24 as well as in the state after annealing at 300 ℃ for 8 h is compared. Two processing routes – cast technique and rolling – influence significantly the yield strength. The observed difference in the yield strength values may be accounted for by the difference in the grain size and mainly by an increase in the dislocation density after rolling.

The shapes of the true stress-true strain curves of samples prepared by both routes are very similar. However, the testing temperature influences significantly the deformation behaviour of AZ31 alloy independent of fabrication technique. The flow stress and strain hardening decrease with increasing temperature. At temperatures above 200–250 ℃, a dynamic balance between hardening and softening takes place; the strain hardening rate is close to zero. The AZ31 sheets in the state after annealing at 300 ℃ for 8 h exhibit lower flow stresses than their counterparts in the H24 state. The lifts in the course of the stress dependence of the strain hardening rate for the annealed sheets are likely connected with dislocation glide in non-basal slip systems. The observed deformation behaviour is discussed from the view of the dislocation motion in different slip planes. Glissile and sessile dislocations are created by an interaction between basal and non-basal slips, which contributes to hardening and softening. The double cross slip of screw components of both <**a**> and <**c** + **a**> dislocations on prismatic planes may cause annihilation of dislocations leading to softening.

Acknowledgements

We would like to dedicate this paper to Ing. Juraj Lapin, DrSc., on the occasion of his 50$^{\mathrm{th}}$ birthday. The authors acknowledge the financial support of the Academy of Sciences of the Czech Republic under Grant IAA201120902.

References

[1] VON MISES, R.: Z. angw. Mat. Mech., *8*, 1928, p. 161.
[2] LUKÁČ, P.: Czech. J. Phys. B, *31*, 1981, p. 135. http://dx.doi.org/10.1007/BF01959434
[3] LUKÁČ, P.: Czech. J. Phys. B, *35*, 1985, p. 275. http://dx.doi.org/10.1007/BF01605096
[4] AGNEW, S. R.—DUYGULU, O.: Int. J. Plasticity, *21*, 2005, p. 1161. http://dx.doi.org/10.1016/j.ijplas.2004.05.018
[5] BARNETT, M. R.: Mater. Sci. Eng. A, *464*, 2007, p. 1. http://dx.doi.org/10.1016/j.msea.2006.12.037
[6] CAILLARD, D.—MARTIN, J. L.: Thermally Activated Mechanisms in Crystal Plasticity. Amsterdam, Pergamon Press 2003.
[7] CÁCERES, C. H.—LUKÁČ, P.: Phil. Mag., *88*, 2008, p. 977.
[8] BALÍK, J.—LUKÁČ, P.—DROZD, Z.—KUŽEL, R.: Int. J. Mat. Res., *100*, 2009, p. 322.
[9] BALÍK, J.—LUKÁČ, P.—BOHLEN, J.—KAINER, K. U.: Kovove Mater., *45*, 2007, p. 135.
[10] HALL, E. O.: Proc. Phys Soc. B, *64*, 1951, p. 747. http://dx.doi.org/10.1088/0370-1301/64/9/303
[11] PETCH, N. J.: J. Iron Steel Inst., *174*, 1953, p. 25.
[12] ONO, N.—NAKAMURA, K.—MIURA, S.: Mater. Sci. Forum, *419–422*, 2003, p. 195. http://dx.doi.org/10.4028/www.scientific.net/MSF.419-422.195
[13] BARNETT, M. R.—KESHAVARZ, Z.—BEER, A. G.—ATWELL, D.: Acta Mater., *52*, 2004, p. 5093. http://dx.doi.org/10.1016/j.actamat.2004.07.015
[14] DEL VALLE, J. A.—CARRENO, F.—RUANO, O. A.: Acta Mater., *54*, 2006, p. 4247. http://dx.doi.org/10.1016/j.actamat.2006.05.018
[15] ZUBEROVA, Z.—SABIROV, I.—ESTRIN, Y.: Kovove Mater., *49*, 2011, p. 29.
[16] TROJANOVÁ, Z.—LUKÁČ, P.: Int. J. Mat. Res., *100*, 2009, p. 270.
[17] ONO, N.—UEDA, M.—MIURA, S.: Mater. Sci. Forum, *488–489*, 2005, p. 355.
[18] MÁTHIS, K.—TROJANOVÁ, Z.—LUKÁČ, P.—CÁCERES, C. H.—LENDVAI, J.: J. Alloys Comp., *378*, 2004, p. 176.
[19] WU, H. Y.—LIN, F. Z.: Mater. Sci. Eng. A, *527*, 2010, p. 1194. http://dx.doi.org/10.1016/j.msea.2009.09.049
[20] MÁTHIS, K.—NYILAS, K.—AXT, A.—DRAGOMIR-CERNATESCU, I.—UNGAR, T.—LUKÁČ, P.: Acta Mater., *52*, 2004, p. 2889.
[21] COURET, A.—CAILLARD, D.: Acta Metall., *33*, 1985, p. 1447. http://dx.doi.org/10.1016/0001-6160(85)90045-8
[22] COURET, A.—CAILLARD, D.: Acta Metall., *33*, 1985, p. 1455. http://dx.doi.org/10.1016/0001-6160(85)90046-X
[23] LUKÁČ, P.—BALÍK, J.: Key Eng. Mater., *97–98*, 1994, p. 307.